Evidence for the distortion product frequency place as a source of distortion product otoacoustic emission (DPOAE) fine structure in humans. I. Fine structure and higher-order DPOAE as a function of the frequency ratio $f2/f1$ [a)]

Manfred Mauermann[b)] and Stefan Uppenkamp[c)]
AG Medizinische Physik, Universität Oldenburg, D-26111 Oldenburg, Germany

Peter W. J. van Hengel
BCN, Rijksuniversiteit Groningen, 9747 AG Groningen, The Netherlands

Birger Kollmeier
AG Medizinische Physik, Universität Oldenburg, D-26111 Oldenburg, Germany

(Received 10 January 1999; accepted for publication 24 August 1999)

Critical experiments were performed in order to validate the two-source hypothesis of distortion product otoacoustic emissions (DPOAE) generation. Measurements of the spectral fine structure of DPOAE in response to stimulation with two sinusoids have been performed with normal-hearing subjects. The dependence of fine-structure patterns on the frequency ratio f_2/f_1 was investigated by changing f_1 or f_2 only (fixed f_2 or fixed f_1 paradigm, respectively), and by changing both primaries at a fixed ratio and looking at different order DPOAE. When f_2/f_1 is varied in the fixed ratio paradigm, the patterns of $2f_1-f_2$ fine structure vary considerably more if plotted as a function of f_2 than as a function of f_{DP}. Different order distortion products located at the same characteristic place on the basilar membrane (BM) show similar patterns for both, the fixed-f_2 and f_{DP} paradigms. Fluctuations in DPOAE level up to 20 dB can be observed. In contrast, the results from a fixed-f_{DP} paradigm do not show any fine structure but only an overall dependence of DP level on the frequency ratio, with a maximum for $2f_1-f_2$ at f_2/f_1 close to 1.2. Similar stimulus configurations used in the experiments have also been used for computer simulations of DPOAE in a nonlinear and active model of the cochlea. Experimental results and model simulations give strong evidence for a two-source model of DPOAE generation: The first source is the initial nonlinear interaction of the primaries close to the f_2 place. The second source is caused by coherent reflection from a re-emission site at the characteristic place of the distortion product frequency. The spectral fine structure of DPOAE observed in the ear canal reflects the interaction of both these sources. [S0001-4966(99)02812-X]

PACS numbers: 43.64.Jb, 43.64.Kc [BLM]

INTRODUCTION

Narrow-band distortion product otoacoustic emissions (DPOAE) are low-level sinusoids recordable in the occluded ear canal at certain combination frequencies during continuous stimulation with two tones. They are the result of the nonlinear interaction of the tones in the cochlea. In human subjects, DPOAE typically exhibit a pronounced spectral fine structure when varying the frequencies of both primaries simultaneously (f_1,f_2) at a fixed frequency ratio f_2/f_1 (Gaskill and Brown, 1990; He and Schmiedt, 1993). The variations of DPOAE level with frequency show a periodicity of about 3/32 octaves (He and Schmiedt, 1993; Mauermann *et al.*, 1997b) in a depth up to 20 dB. DPOAE can be recorded in almost any normal-hearing subject and in subjects with hearing loss up to 50 dB HL (Smurzynski *et al.*, 1990). Because of the narrow-band nature of both stimuli and emissions, they provide a frequency-specific method to explore cochlear mechanics. Therefore, DPOAE are of great interest not only in laboratory studies but also as a diagnostic tool for clinical audiology. However, since it is not as yet completely understood which sources along the cochlear partition contribute to the emission measured in the ear canal, the applicability of DPOAE for, e.g., ''objective'' audiometry is limited at present.

For DPOAE with frequencies below the primary frequencies ($2f_1-f_2$,$3f_1-2f_2$, etc.), it is widely accepted that the generation site is the overlap region of the excitation patterns of the two primaries, which has a maximum close to the characteristic site around f_2. Although the generation of distortion products due to the interaction of the two primaries is in principle spread over the whole cochlea, a region of about 1 mm around the characteristic place of f_2 has been suggested to give the maximum contribution (van Hengel and Duifhuis, 1999). This region of maximum contribution is referred to as the f_2 site.

[a)]Parts of this study were presented at the 1998 short papers meeting of the British Society of Audiology in London [Uppenkamp and Mauermann, Br. J. Audiol. **33**, 87–88 (A) (1999)].

[b)]Author to whom correspondence should be addressed. Electronic mail: mani@medi.physik.uni-oldenburg.de

[c)]Current address: CNBH, Department of Physiology, University of Cambridge, Downing Street, Cambridge CB2 3EG, U.K.

It is still a point of discussion whether the generation site is the only source or to what extent other sources might also contribute to the emission. The DPOAE fine structure found in human subjects is closely related to this question of DPOAE sources. The fine structure might reflect local BM properties of either the generation site or of the re-emission site. It could also result from the interference between two or more sources or even from a combination of both local properties and interference effects. Studying the properties of DPOAE fine structure may result in further insight into BM mechanisms and the location of DP sources.

The patterns of DPOAE fine structure get shifted along the frequency axis when the primary levels are increased (He and Schmiedt, 1993; Mauermann *et al.*, 1997b) or the frequency ratio of the primaries is changed (Mauermann *et al.*, 1997a). On one hand, these shifts may cause some problems in the interpretation of DPOAE measurements, especially DPOAE growth functions. Peaks may change to notches or vice versa. This is most probably the reason for the notches found in human DPOAE growth functions (He and Schmiedt, 1993) and is critical for a direct correlation of DPOAE level to hearing threshold. On the other hand, the correct interpretation of these fine-structure shifts can aid in a detailed understanding of BM mechanisms.

He and Schmiedt (1993) showed that the level-dependent shift of DPOAE fine structure is consistent with the results of Ruggero and Rich (1991) on the shift of the maximum basilar-membrane response in the chinchilla. They interpreted the fine structure as an effect of local BM properties in the region of the primaries and the level-dependent shift as a result of the shift of the primary excitation on the BM (He and Schmiedt, 1993; Sun *et al.*, 1994a, b). Varying only one primary level while holding the other fixed causes pattern shifts in different directions, dependent on whether the primary level at f_1 or at f_2 is varied. He and Schmiedt (1997) argued that these effects strongly support the idea that the DPOAE fine structure might reflect mechanical properties of the overlapping area of the primary excitation.

However, Heitmann *et al.* (1998) showed that the fine structure disappears when the DPOAE is measured with a third tone close to the distortion product frequency (f_{DP}) as a suppressor. This result is interpreted as evidence for an additional second source around the characteristic place of $2f_1-f_2$, which has a major influence on the fine-structure pattern. The contribution of a second source at the place of $2f_1-f_2$ is also supported by several experiments on DPOAE suppression. Kummer *et al.* (1995) reported that in some cases a suppressor close to $2f_1-f_2$ results in more suppression than one close to f_2. Gaskill and Brown (1996) also found that the DP level is still sensitive to a suppressor near $2f_1-f_2$, although the major suppression effects they observed were for suppressor frequencies close to f_2. Brown *et al.* (1996) showed ''that it may be legitimate to analyze DP as vector sum of two gross components,'' (Brown *et al.*, 1996, p. 3263).

Throughout the present paper, experimental results from normal-hearing subjects and computer simulations will be presented examining in detail the properties of DPOAE fine structure for equal-level primaries and varied ratios of the primary frequencies. Three ''critical'' experiments have been performed, using different experimental paradigms, that aim to clarify where and how DPOAE fine structure is generated. Experiment 1 investigates DPOAE fine-structure patterns for different f_2/f_1 to determine whether the fine structure is dominated by local properties of the f_2 region or if a supposed re-emission site around f_{DP} is of some importance. Experiment 2 is designed to test the influence of the relative phase between the suggested emission sites by investigating the patterns of different order DPOAE. Finally, in experiment 3 the DPOAE patterns from a f_{DP}-fixed and a f_2-fixed paradigm are compared to find out if DPOAE fine structure is mainly influenced by one of these two sites.

In addition to the recordings from subjects, all experimental paradigms were also assessed with a computer simulation of DPOAE using a nonlinear and active transmission line model of the cochlea. This model includes an impedance function as suggested by Zweig (1991) which produces excitation patterns with a broad and tall peak. Within the model, statistical fluctuations of stiffness along the cochlear partition are sufficient to create quasiperiodic OAE fine-structure patterns, as reported by Zweig and Shera (1995).

I. METHODS

A. Subjects

Seven normal-hearing subjects, ranging in age from 25 to 30 years, participated in this study. Their hearing thresholds were better than 15 dB HL for all audiometric frequencies in the range 250 Hz–8 kHz, and none of the subjects had a history of any hearing problems. Spontaneous otoacoustic emissions (SOAE) were observed in only one of the subjects (subject SE). DPOAE were recorded from one ear of each subject during several sessions lasting 60–90 min. During the sessions, the subjects were seated comfortably in a sound-insulated booth (IAC-1200 CT).

B. Instrumentation and signal processing

An insert ear probe, type ER-10C, was used to record DPOAE. The microphone output was connected to a low-noise amplifier, type SR560, and then converted to digital form using the 16-bit A/D converters on a signal-processing board (Ariel DSP-32C) in a personal computer. All stimuli were generated digitally. After D/A conversion by the 16-bit D/A converters on the Ariel board and low-pass filtering (Kemo VBF44, 8.5 kHz) they were presented to the subjects via a computer-controlled audiometer. The DSP was used for on-line analysis and signal conditioning of the recorded emissions, including artifact rejection, averaging in the time domain to improve the signal-to-noise ratio, and fast Fourier transform (FFT). For each signal configuration, at least 16 but usually 256 frames were averaged, using a frame length of 186 ms (4096 samples). If required, the number of averages could be increased during the recording to get a sufficient signal-to-noise ratio for the frequencies of interest.

Two sinusoids were generated as even harmonics of the frame rate (5.38 Hz) at a sampling rate of 22 050 Hz. The tones were presented continuously to the subject. To compensate for the ear-canal transfer function, an individual ad-

justment of the primaries to the desired sound-pressure level of 60 dB SPL was performed automatically before each run, taking into account the transfer function of the probe microphone. The variations of attenuation within and between subjects were approximately within a range of 5 dB.

C. Experimental paradigms

1. Dependence of the $2f_1-f_2$ DPOAE on frequency ratio

In experiment 1, the effect of the frequency ratio f_2/f_1 on the fine-structure patterns of the DPOAE at $2f_1-f_2$ was investigated. Fine-structure patterns for this distortion product were recorded in all subjects for seven different frequency ratios f_2/f_1, fixed at 1.07, 1.1, 1.13, 1.16, 1.19, 1.22, and 1.25. Due to the additional requirement to select the primaries as harmonics of the frame rate, minor deviations up to 0.002 from the desired frequency ratio were present. Recordings were taken covering a frequency range of two octaves ($f_2=1-4$ kHz), divided into four sessions covering half an octave each for all of the different frequency ratios specified above. The frequency step between adjacent single recordings was 1/48 octave.

It is assumed that the small changes in the frequency ratio cause only small changes in the fine-structure patterns, i.e., the patterns remain comparable. Consequently, if the fine-structure patterns are mostly influenced by the local properties of the generation site near the characteristic place of f_2, the patterns for different f_2/f_1 should show a high stability when plotted as a function of f_2. If, however, the local properties of a presumed re-emission site near the characteristic place of the DPOAE frequency play a major role, the stability of the patterns should be greater when plotted as a function of f_{DP}.

2. Different order DPOAE

In experiment 2, fine-structure patterns for different order DPOAE (e.g., $2f_1-f_2$, $3f_1-2f_2$, and $4f_1-3f_2$) were recorded from six of our seven subjects. The frequency ratios were chosen to get identical frequency pairs either for f_2 and $2f_1-f_2$, f_2 and $3f_1-2f_2$, and f_2 and $4f_1-3f_2$, or for f_1 and $2f_1-f_2$, f_1 and $3f_1-2f_2$, and f_1 and $4f_1-3f_2$, respectively. The condition for identical f_2 and f_{DP} frequencies is fulfilled for the frequency ratios $f_2/f_1=1.22$, 1.137, and 1.099. Similarly, the required identity of f_1 and f_{DP} frequencies is fulfilled at frequency ratios $f_2/f_1=1.22$, 1.11, and 1.073 (see Fig. 1).

If the DPOAE fine structure is mainly caused by two sources, one at the generation site and the other one at the distortion frequency site, measurements for different order DPOAE with identical f_2 and f_{DP} frequencies should result in very similar patterns, since both f_2 and the observed DP frequency are the same, i.e., the characteristic places of the two assumed sources and hence the phase relation between the two is almost identical (see Fig. 1, left column). With identical f_1 and f_{DP} frequencies, a small variation in the pattern is expected, indicating the influence of the change in the relative phase of the f_2 and f_{DP} components (see Fig. 1, right column).

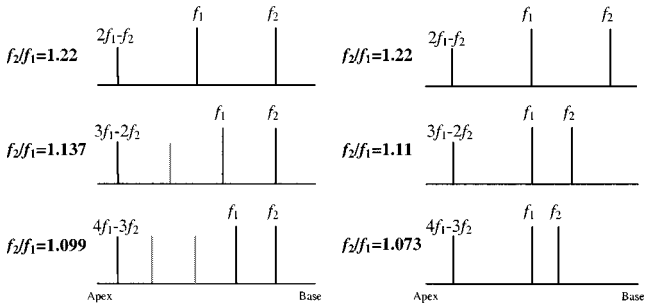

FIG. 1. Sketch of stimulus configuration for the comparison of different order DPOAE fine-structure patterns. For the condition of identical f_2 and f_{DP} frequencies, f_2/f_1 was set to 1.22, 1.137, and 1.099 to get identical DP frequencies $f_{DP}=0.64f_2$ for $2f_1-f_2$, $3f_1-2f_2$, and $4f_1-3f_2$, respectively. Similarly, to fulfill the condition of identical f_1 and f_{DP} frequencies, f_2/f_1 was set to 1.22, 1.11, and 1.073, resulting in $f_{DP}=0.78f_1$.

3. Fixed f_2 vs fixed f_{DP}

An additional test for investigating the source of the fine structure was performed during experiment 3. DPOAE were recorded in keeping either f_{DP} or f_2 fixed. This was achieved by varying both f_1 and f_2 while keeping f_{DP} fixed at 2 kHz or varying f_1 and keeping f_2 fixed at 3 kHz resulting in varying f_{DP}. Both paradigms result in a varying frequency ratio f_2/f_1.

The comparison of the two paradigms should reveal the relative contribution of the two supposed sources. If the fine-structure pattern of the DPOAE is dominated by the contribution from the characteristic place of the distortion product frequency, it is expected that the observable pattern shows much less variation between minima and maxima when f_{DP} is held constant.

D. Analysis

For further analysis, the frequencies in all experiments were transformed to their characteristic places $x(f)$ on the BM using the place–frequency map proposed by Greenwood (1991). Although the frequencies used are almost equally spaced on the Greenwood map, there are some deviations from this. These deviations are mainly due to the fact that the primaries were selected as harmonics of the frame rate. To compensate for that, the data were interpolated using a cubic spline algorithm (MATLAB 5.1) and resampled at 1024 points equally spaced on the Greenwood map. Cross-correlation functions (CCF) were calculated using the data from experiment 1 to quantify the shift between two different fine-structure patterns. The correlation lag giving the maximum of the CCF within the range ± 1 mm was taken as shift between two fine-structure patterns with adjacent frequency ratios. It is assumed that small changes in frequency ratio will cause only small shifts of the overall fine structure. Therefore, the range to look for maxima of the CCF was limited to avoid ambiguities which could be caused by the quasiperiodic shape of the patterns. The computation of CCF was always restricted to the area of actual overlap between the compared patterns.

II. EXPERIMENTAL RESULTS

A. Experiment 1: Dependence on f_2/f_1

Figure 2 shows the effect of variation of f_2/f_1 (seven different f_2/f_1 ratios) on the DP fine-structure patterns for the $2f_1-f_2$ distortion product for four different subjects. The left column shows the results plotted as a function of f_2 place, and the right column shows the same data as a function of $2f_1-f_2$. The labeling of the ordinate holds for the bottom trace only . Each successive trace that corresponds to a different f_2/f_1 ratio is shifted by 20 dB. Note the pronounced shift in the basal direction of successive patterns when plotted as a function of f_2. This contrasts with the small shift in the apical direction when plotted as a function of $2f_1-f_2$. This is illustrated by the lines in the middle column showing the cumulative sum of correlation lag for the maxima in the CCF between successive patterns. The similarity between adjacent patterns is relatively high for small differences in f_2/f_1. However, the patterns become more different when the changes in frequency ratio get bigger.

B. Experiment 2: Fine structure of different order DPOAE

Figure 3 shows fine-structure patterns for different order DPOAE characterized by the same distance along the basilar membrane between f_2 and f_{DP} (right column) or f_1 and f_{DP} (left column) for the same four subjects as in Fig. 2. As Fig. 3 illustrates, the patterns for same f_2 and f_{DP} frequencies are very similar, suggesting that the relative phase between the DP components contributing from the characteristic places of f_2 and f_{DP} plays an important role in the DPOAE fine structure. For identical f_1 and f_{DP} the patterns still look similar. However, for most of the subjects the CCF indicates a slight shift in the basal direction for the higher-order DPOAE. This is consistent with the movement of the f_2 place in the apical direction with increasing order in this case.

C. Experiment 3: Fixed f_2 vs fixed f_{DP}

While the results from experiments 1 and 2 indicate that the DPOAE observed in the human ear canal stems from two sources along the cochlea partition, one close to the f_2 site and one at the f_{DP} site, a separation of the contribution of these two sources cannot be achieved using these data. Figure 4 shows DPOAE patterns for four subjects (two of them as in Figs. 2 and 3) obtained with a fixed f_2 (gray line) and with a fixed f_{DP} (black line). The use of a fixed f_2 results in patterns very similar to the ones observed before, using the fixed-ratio paradigm. In contrast, the use of a fixed f_{DP} greatly reduces the fine structure. There remains only an overall dependence of DP level on frequency ratio, with a maximum for $2f_1-f_2$ at f_2-f_1 around 1.2, as reported, e.g., by Harris *et al.* (1992).

III. SIMULATIONS IN A NONLINEAR AND ACTIVE COCHLEA MODEL

A. Description of the model

For computer simulations of the observed effects, a one-dimensional nonlinear and active model of the cochlea was used, based on a model described in previous work (van Hengel *et al.*, 1996; van Hengel and Duifhuis, 1999). In these papers it was shown that the model, which operates in the time domain, is very useful to study nonlinear phenomena such as OAE. The basis for such models has been described in more detail in Duifhuis *et al.* (1985) and van den Raadt and Duifhuis (1990). In previous simulations of DPOAE, it turned out that a possible shortcoming of the model was that it did not produce a high and broad excitation peak for pure-tone stimuli (van Hengel and Duifhuis, 1999). It is claimed by various authors that such a peak is necessary to properly simulate cochlear behavior at low stimulus levels (e.g., Zweig, 1991; de Boer, 1995). Furthermore, it was claimed by Shera and Zweig (1993) and shown by Talmadge *et al.* (1993, 1998) that the impedance function suggested by Zweig (1991), which produces a high and broad excitation peak, also produces a fine structure in various types of simulated emissions when it is combined with a ''roughness'' in the mechanical parameters of the cochlear partition. This roughness is a random fluctuation of (one of) the parameters describing the mechanics of the sections of the cochlear partition used in the model, and reflects random inhomogeneity in the placement and behavior of cells along the cochlea, especially the outer hair cells. The impedance function described by Zweig (1991) was therefore incorporated in the model, as well as the possibility of introducing roughness. The resulting model consists of 600 sections[1] equally spaced along the length of the cochlea (35 mm). The motion of the cochlear partition in each section is described by the following equation of motion:

$$m\ddot{y}(x)+d(x,v)\dot{y}(x)+s(x)[y(x)+c(v)y(x)|_{t-\tau}]=p(x). \tag{1}$$

This is a normal second-order differential equation of motion for a harmonic oscillator with mass m, damping $d(x,v)$, and stiffness $s(x)$, driven by a pressure force $p(x)$ (x is the position of the oscillator measured from the stapes along the cochlea, y is the displacement, and $v=\dot{y}$ the velocity of the cochlear partition in the vertical direction), except that there is an additional ''delayed feedback stiffness'' term $s(x)c(v)y(x)|_{t-\tau}$. This term was derived by Zweig (1991) from fits to experimental data on BM excitation patterns. It serves to stabilize the motion of the oscillator, counteracting a negative damping term $d(x,v)$. In order to do so, and to arrive at the desired high and broad peak in the excitation caused by a pure tone, the time delay τ must depend on the resonance frequency $\omega_{res}=\sqrt{s(x)/m}$ of the oscillator as $\tau=1.742\times 2\pi/\omega_{res}$ (Zweig, 1991). The values of the parameters $d(x,v)$ and $c(v)$ determined by Zweig were $-0.1217\sqrt{ms(x)}$ and 0.1416, respectively. It is important to note that these values are derived from estimated excitation patterns in the cochlea of the squirrel monkey at low levels of stimulation and in the frequency range around 8 kHz.

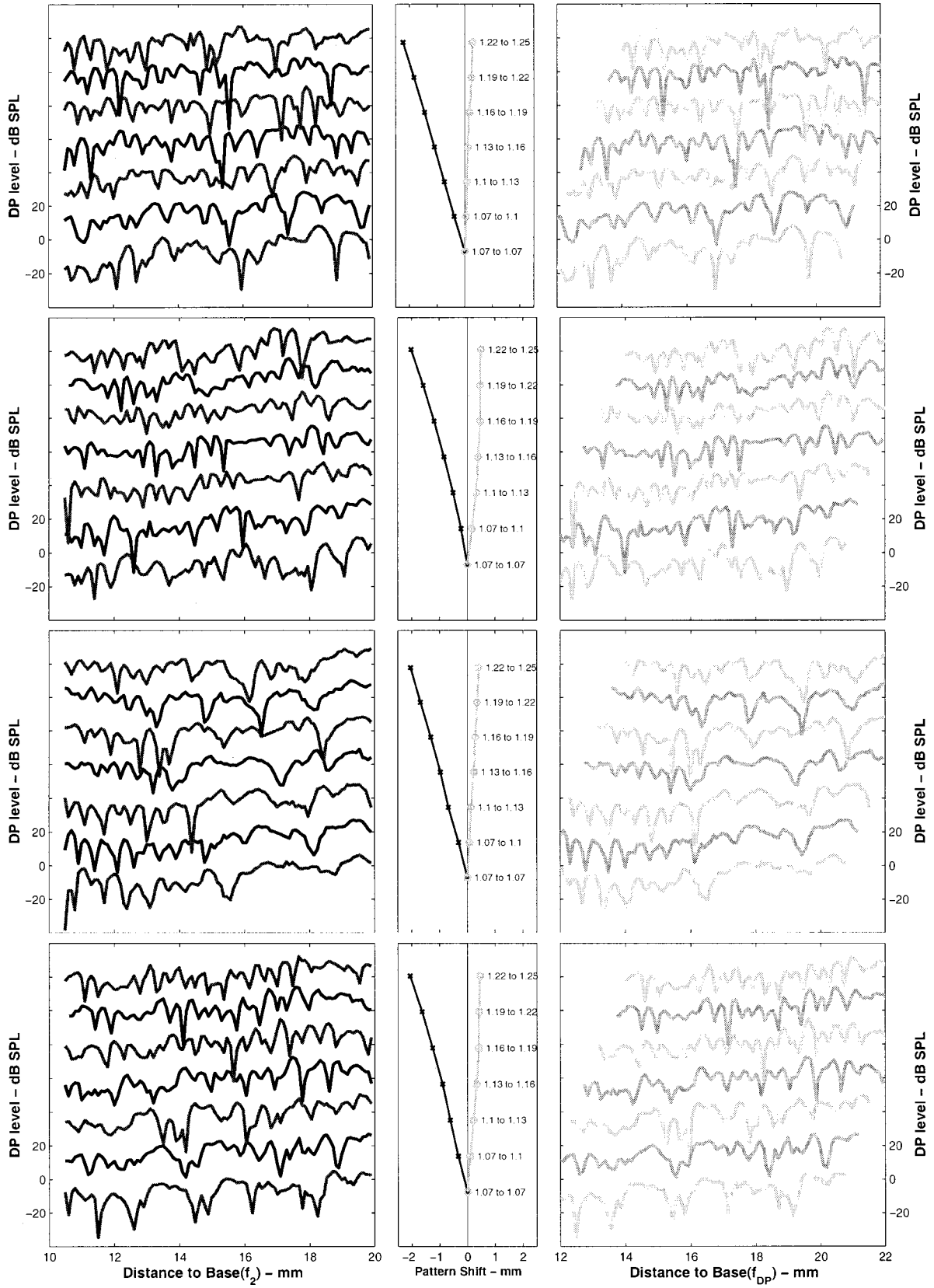

FIG. 2. Experiment 1: Dependence of $2f_1-f_2$ DPOAE fine structure on the frequency ratio f_2/f_1 for four different subjects (from top to bottom: KI right, MG left, MK right, and MM right). Each row shows DPOAE fine-structure patterns for seven different ratios f_2/f_1 (from bottom to top: 1.07, 1.1, 1.13, 1.16, 1.19, 1.22). Left column: DP level as a function of f_2 place. 10-mm distance to base corresponds to a frequency $f_2=4358$ Hz, and 20 mm distance corresponds to $f_2=986$ Hz. Right column: same data as a function of $2f_1-f_2$. 12 mm corresponds to $f_{DP}=3270$ Hz, and 22 mm corresponds to $f_{DP}=713$ Hz. The labeling of the ordinate holds for the bottom trace only. Each successive trace is shifted up by 20 dB. Middle column: shift between the different DPOAE patterns when plotted as a function of f_2 (black line) and when plotted as a function of $2f_1-f_2$ (gray line). This overall shift is quantified by the correlation lag for the maximum of the cross-correlation function between adjacent patterns. Each data point results from cumulative summation of the shifts between adjacent patterns (as indicated by the numbers ''1.07 to 1.1,'' ''1.1 to 1.13,'' etc.), starting at the frequency ratio 1.07.

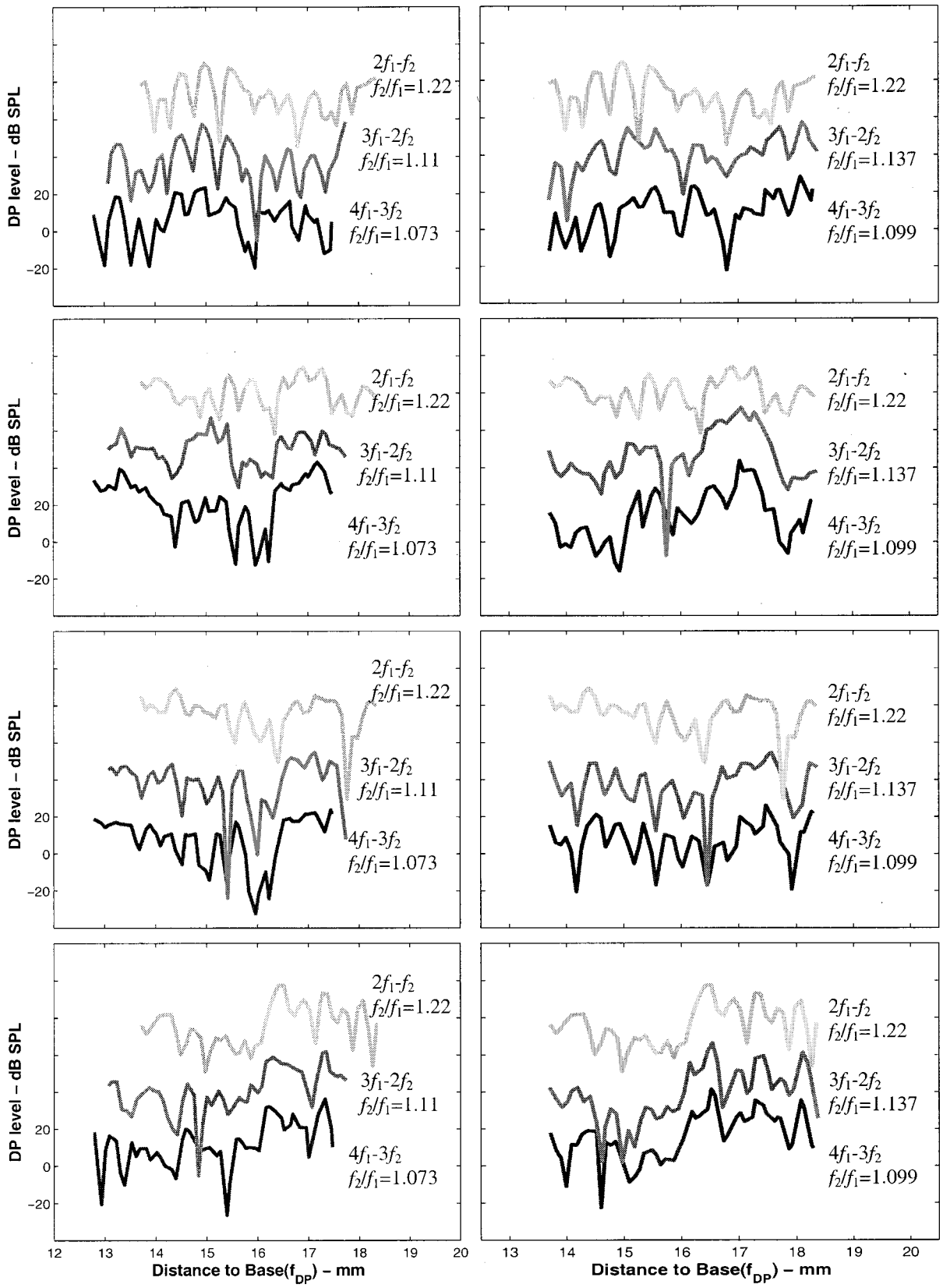

FIG. 3. Experiment 2: Comparison of different order DPOAE fine-structure patterns for four subjects. Left column: Identical f_1 and f_{DP} frequencies, right column: Identical f_2 and f_{DP} frequencies. The frequency ratios f_2/f_1 were chosen according to the scheme in Fig. 1. Note the very similar patterns for all orders of DPOAE. The labeling of the ordinate holds for the bottom trace only. Each successive trace is shifted by 20 dB. 13 mm corresponds to f_{DP}=2830 Hz. Same subjects as in Fig. 2.

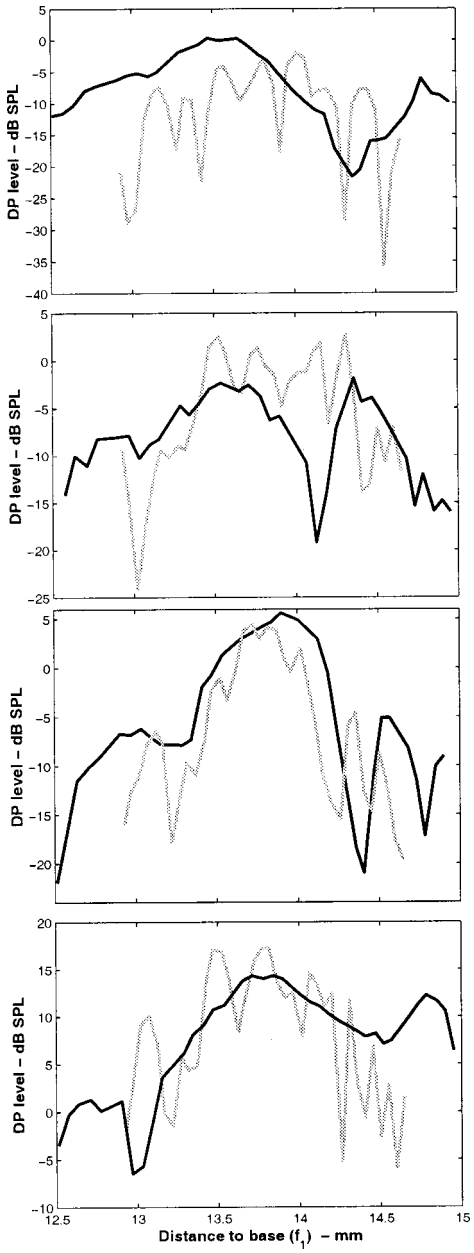

FIG. 4. Experiment 3: DP level as a function of f_1 for four subjects. Black lines: fixed-f_{DP} paradigm, i.e., varying both f_1 and f_2 while keeping f_{DP} fixed at 2 kHz. Gray lines: fixed-f_2 paradigm, i.e., varying f_1 and f_{DP} while f_2 is fixed at 3 kHz. Note the fine structure for the fixed-f_2 paradigm, which is similar to the patterns observable with the fixed-ratio paradigm, while there is no fine structure when using the fixed f_{DP} paradigm. Subjects from top to bottom: MK right, MM right, OW right, and SE right.

These values certainly cannot be used in the vicinity of both stapes and helicotrema, since this would lead to instability (van Hengel, 1993). It is also clear that these values do not hold for higher stimulus levels. Both the negative damping term and the stabilizing delayed feedback stiffness term are thought to result from active, i.e., energy producing, behavior of the outer hair cells. This active behavior must saturate at higher levels. It is therefore logical to capture the nonlinearities present in cochlear mechanics in the terms $d(x,v)$ and $c(v)$.[2] The nonlinearity was introduced by assuming the following dependence of $d(x,v)$ and $c(v)$ on the velocity v of the section:

$$d(x,v)=\left[d_l+\frac{\beta(d_h-d_l)|v|}{1+\beta|v|}\right]\sqrt{ms(x)}$$

$$\text{with } d_l=-0.12,\ \ d_h=0.5, \tag{2a}$$

$$c(v)=c_l+\frac{-\beta d_l|v|}{1+\beta|v|}\quad c_l=0.1416. \tag{2b}$$

In these equations the nonlinear behavior of $d(x,v)$ and $c(v)$ is chosen to be the same, with the damping going to a value of $d_h\sqrt{ms(x)}$ and the delayed feedback stiffness disappearing at high excitation levels. The region in which the nonlinearity plays a role is determined by the parameter β. In all simulations presented here, a value of 0.01 ms/nm was used for this parameter, leading to a compressive growth of the excitation at the characteristic place for a pure-tone stimulus of around 0.3 dB/dB over the range from about 20 to 80 dB SPL stimulus level. Because the mass m was chosen to be 0.375 kg/m^2, independent of the position x, the stiffness controls the place–frequency map of the cochlear partition. The place–frequency map chosen was

$$f(x)=A\times e^{-ax},\quad A=22.508\ \text{kHz},\quad a=150\,\text{m}^{-1}. \tag{3}$$

Following the work of Shera and Zweig (1993) and Talmadge and Tubis (1993), the random fluctuations necessary to obtain a fine structure in the emissions were introduced in the stiffness as

$$s(x)=s(x)[1+r_0r(x)], \tag{4}$$

where $r(x)$ is a random variable with a Gaussian distribution and r_0 is a scaling parameter that controls the amount of roughness. For the results presented here, a value of 1% was used for r_0. The equations of motion [Eq. (1)] for all sections were coupled through the fluid, which was assumed linear, incompressible, and inviscid. The coupled system was solved by Gauss elimination and integrated in time using a Runge–Kutta 4 time-integration scheme with a sampling frequency of 150 kHz. Reducing the sampling frequency could lead to instabilities in certain cases, but increasing it did not give significantly different results (differences in emission levels were below 0.5%).

To simulate OAE, the motion of the cochlea sections is coupled to the outside world via a simplified middle ear, consisting of a mass, stiffness, and damping in combination with a transformer. This produces a sound pressure that would result at the eardrum in an open ear canal. Previous studies with this model have shown that emission levels are highly sensitive to conditions at the eardrum. SOAE level may vary up to 30 dB when different loading impedances are added (van den Raadt and Duifhuis, 1993).

B. Simulations

All the experiments described in Sec. II (except experiment 2 for the condition of same f_1 and f_{DP} frequencies) were simulated using this computer model. In contrast to the experiments, all simulations were performed with primary levels of 50 dB SPL. The model output is the sound-pressure level at the eardrum taken from a 30-ms interval beginning 20 ms after stimulus start to avoid onset effects. The data

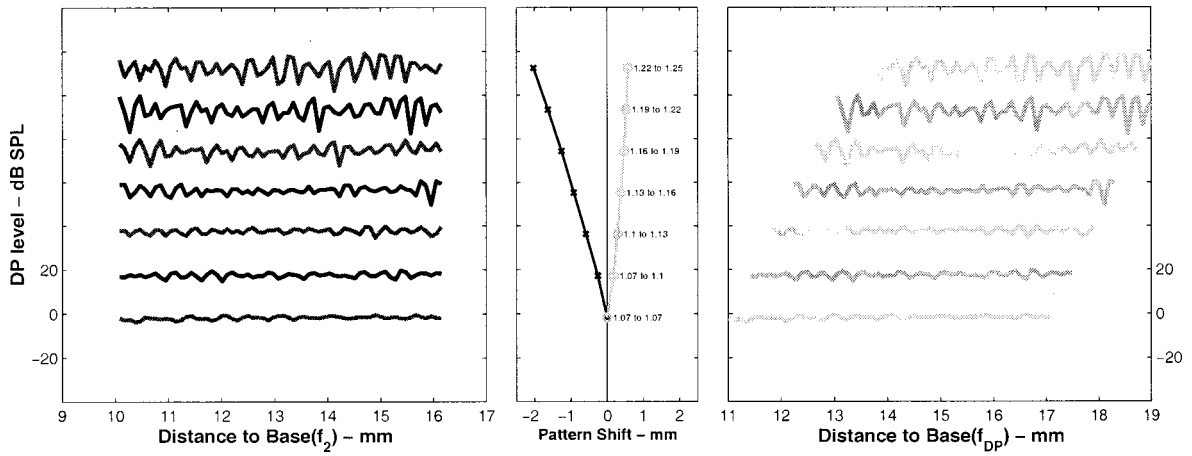

FIG. 5. Computer simulation of experiment 1: Dependence of $2f_1-f_2$ DPOAE fine structure on the frequency ratio f_2/f_1. Left column: DP level as a function of f_2 place. 10 mm distance to base corresponds to a frequency $f_2=5027$ Hz, and 16-mm distance corresponds to $f_2=2045$ Hz, according to the exponential place–frequency map used in the cochlea model. Right column: same data as a function of $2f_1-f_2$ place. 11 mm corresponds to $f_{DP}=4327$ Hz, and 19 mm corresponds to $f_{DP}=1304$ Hz. As in Fig. 2, the shift between adjacent patterns is illustrated by the lines in the middle column of the figure based on cross correlation.

were analyzed using the least-squares-fit method described by Long and Talmadge (1997) to get an estimate of the spectral power of the frequency components of interest. The further analysis of pattern shifts was performed using cross correlation as described for the experimental data.

The simulation results are given in Figs. 5–7. Analogous to the experimental data in Fig. 2, Fig. 5 shows simulated DPOAE fine-structure patterns for different frequency ratios of the primaries plotted as a function of f_2 (left panel) and f_{DP} (right panel). The main experimental result, i.e., the shift of fine-structure patterns when varying the frequency ratio, is replicated very well, both qualitatively and quantitatively. Figure 6 shows fine-structure patterns for three different frequency ratios, which were chosen to get the same frequencies for f_2 and $2f_1-f_2$, $3f_1-2f_2$, or $4f_1-3f_2$, respectively. As in the experiments, the patterns for different order DPOAE were almost identical in all these stimulus conditions. Figure 7 shows that, in the model, the fine structure disappears in a fixed f_{DP} paradigm, similar to the experimental results, while the model still produces a fine structure for fixed f_2. The only discrepancies between simulations and experimental results in the fine structure are the reduced dynamical range between maxima and minima in the model for small frequency ratios and the slightly smaller period of the frequency-dependent level variations.[3]

Simulations have also been performed omitting the roughness in the model's stiffness function in either (1) the frequency region above 2 kHz, or (2) below 2 kHz, or (3) with no roughness at all, to get a better understanding of the mechanism creating the fine structure in the model. DPOAE with a high frequency resolution were computed over a frequency range for f_2 from 2483 to 3084 Hz at a frequency ratio $f_2/f_1=1.22$. This ensured that the characteristic places of f_{DP} always fell in model sections with characteristic frequencies below 2 kHz, while the characteristic frequencies of

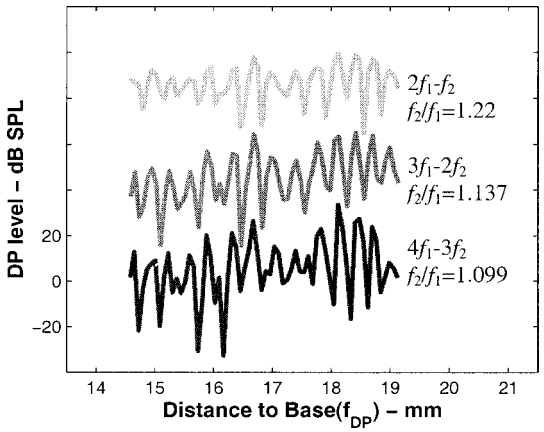

FIG. 6. Computer simulation of experiment 2: Comparison of different order DPOAE fine-structure patterns for identical f_2 and f_{DP} frequencies. The frequency ratios f_2/f_1 were chosen according to the scheme in Fig. 1. Note the very similar patterns for all orders of DPOAE. The labeling of the ordinate holds for the bottom trace only. Each successive trace is shifted by 20 dB. 14 mm corresponds to $f_{DP}=2760$ Hz, according to the exponential frequency map used in the model.

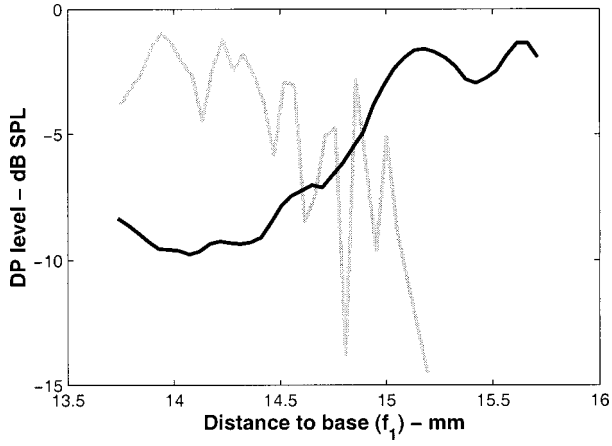

FIG. 7. Computer simulation of experiment 3: DP level as a function of f_1. Black line: fixed f_{DP} paradigm, i.e., varying both f_1 and f_2 while keeping f_{DP} fixed at 2 kHz. Gray line: fixed f_2 paradigm, i.e., varying f_1 and f_{DP} while f_2 is fixed at 3 kHz. Note that, as for the experimental results, the fine structure for the fixed-f_2 paradigm is similar to the patterns observable with the fixed-ratio paradigm, while there is no fine structure when using the fixed-f_{DP} paradigm.

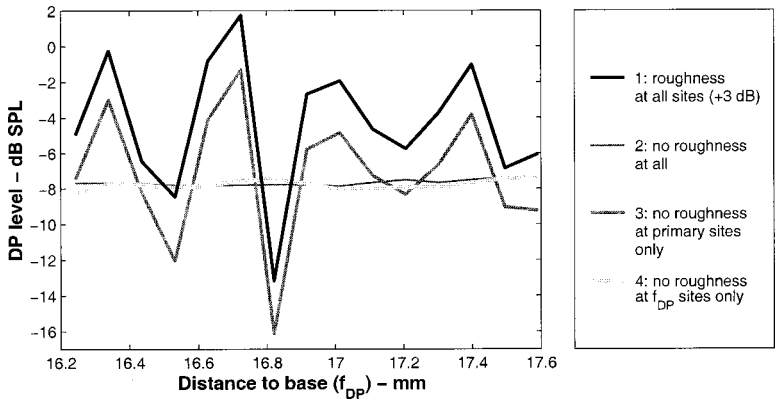

FIG. 8. Computer simulations at a frequency ratio $f_2/f_1=1.22$, but omitting the roughness in different parts of the model cochlea. The primary levels were $L_1=L_2=50$ dB SPL. Line 1 is the reference simulation, a DPOAE fine structure for roughness over the whole cochlea (shifted 3 dB up). Line 2 shows the DPOAE levels for a model cochlea without any roughness in the stiffness function. No fine structure can be observed here. Line 3 shows the DPOAE fine structure using a model cochlea without any fine structure in the region of the primaries. This has no effect on the fine structure, which is almost identical to that for the reference simulation. Line 4 shows DPOAE levels produced by a model cochlea with no roughness at the f_{DP} sites only and the same roughness as in the reference in the primary region. Note that for this condition the DPOAE fine structure disappears completely.

the primaries always fell into sections above 2 kHz. Figure 8 shows the simulation results in these three conditions as well as in the reference condition with roughness over the whole length of the cochlea. The DPOAE fine structure is unaffected by the presence or absence of the roughness in the primary region, while it disappears when the roughness is omitted in the distortion product frequency region. This emphasizes the interpretation of the experimental results that the DPOAE fine structure is mainly influenced by the re-emission components from the characteristic DP places, while emission from the primary component places is almost constant in level and phase over frequency.

IV. DISCUSSION

Similar to recent experimental and theoretical studies on DPOAE fine structure by other authors (e.g., Mauermann *et al.*, 1997a; Heitmann *et al.*, 1998; Talmadge *et al.*, 1998, 1999), our experiments and simulations give further evidence that the fine structure is the result of two sources. Furthermore, the idea is supported that the underlying physical mechanisms of these two sources are different or at least act in a different way (e.g., Shera and Guinan, 1999).

To illustrate this, the results presented in this paper will be interpreted in three steps. The results of experiment 1 show that the DPOAE fine structure is not caused by local mechanical properties of the primary region, but rather that the characteristic site of the distortion product frequency plays a crucial role. Experiment 2 shows that independent of the distortion product order, fine-structure patterns are very similar as long as the characteristic sites of f_2 and of the DP frequencies are the same, i.e., the relative phase between the two emission sites is almost constant in this experiment. Taken together with the findings from experiment 1, this implies that the emission recorded in the ear canal is the vector sum of components from these two sites. The relative phase of these components has at least some influence on the DPOAE fine-structure pattern.

The results of experiment 3 show a quasiperiodic variation when the re-emission site is varied in frequency monotonically while the generation site is held fixed, whereas the quasiperiodic variation in DP level disappears in the case of a fixed re-emission site and a sweep of the f_2 frequency. In terms of a vector summation of two components, this indicates that the component generated at the primary place must be almost constant in level and phase (at least locally) regardless of the frequency. To explain the quasiperiodic variations in the sum of the two components, we have to assume that the re-emission component varies either in phase or in level with increasing frequency. Shera and Zweig (1993) showed that the fine structure of stimulus frequency otoacoustic emissions (SFOAE) can be interpreted as interference of the incoming and outgoing traveling waves with a periodic rotating phase of the cochlear reflectance. It appears reasonable to treat the DPOAE re-emission component in a similar way to SFOAE generation. Therefore, a periodically varying phase of the re-emission component is the most likely explanation for the DPOAE fine structure. Following, furthermore, the arguments of the ''Gedankenexperiment'' described by Shera and Guinan (1998), the different characteristics of the two components (rotating phase of the f_{DP} component, almost constant phase of the f_2 component) indicate that the underlying mechanisms for these two DPOAE components are different. These authors (Shera and Guinan, 1998, 1999) distinguished two classes of OAE mechanisms, ''linear coherent reflection'' and ''nonlinear distortion,'' whereby DPOAE are a combination of both a nonlinear distortion at the generation site and a coherent reflection from the characteristic site of f_{DP}.

The disappearance of fine structure during the fixed f_{DP} experiment shows that there is no coherent reflection from the primary region because there is no rotating phase with frequency. Using the approach suggested by Zweig and Shera (1995) to explain the spectral periodicity of reflection emissions, this had to be expected because the traveling wave from the initial generation site results in constant wavelength only around the f_{DP} site but not in the region around the primaries. Therefore, the contribution from the primary region needs to be generated in a different way,

most probably due to nonlinear distortion. This interpretation of the experiments is confirmed by the computer simulations, which show no effect on the fine structure when removing the roughness (which is necessary for coherent reflections) from the primary region, while the fine structure disappears in simulations when removing the roughness only around the f_{DP} region (see Fig. 8).

The overall good correspondence between simulations and experimental results gives further confirmation for a whole class of two-source interference models like the one used here. This class of models was recently described in detail by Talmadge *et al.* (1998). The simulations with partly removed roughness (see Fig. 8) cannot directly be transformed into an experimental approach because it is impossible to ''flatten out'' certain areas of the human cochlea. But, a situation close to that might be studied. If a local area of the cochlea is damaged, most probably no broad and tall excitation pattern can be built up there, which in addition to roughness is necessary for coherent reflections (Zweig and Shera, 1995; Talmadge *et al.*, 1999). To get further insight into the mechanisms of DPOAE fine structure, this approach is investigated in the accompanying paper (Mauermann *et al.*, 1999) by looking at the DPOAE fine structure of subjects with frequency-specific hearing losses.

V. CONCLUSIONS

Distortion products recorded in the ear canal cannot be traced back to one single source on the basilar membrane. Instead, DPOAE fine structure reflects the interaction of two components with different underlying physical principles. The first component is due to nonlinear distortion at the primary site close to f_2 and has a nearly constant phase and level. The second component is caused by a coherent reflection from the re-emission site at the characteristic place of f_{DP} and shows a periodically varying amplitude or phase when changing the primary frequencies.

ACKNOWLEDGMENTS

This study was supported by Deutsche Forschungsgemeinschaft, DFG Ko 942/11-2. Many fruitful discussions with G. Long, C. Talmadge, and H. Duifhuis, as well as helpful comments by B. Moore on an earlier version of the manuscript, are gratefully acknowledged.

[1]The number of sections had to be increased from the original 400 to at least 600 in order to avoid ''wiggles'' in the excitation patterns. These ''wiggles'' were also found by Talmadge and Tubis in their work on a time-domain model involving the ''Zweig-impedance'' and made them use a spatial discretisation of 4000 sections (Talmadge and Tubis, 1993; and personal communication).

[2]Of course, other terms could also contain nonlinearity. For example, Furst and Goldstein (1982) argue that the stiffness term should be made nonlinear. For reasons of simplicity only $d(x,v)$ and $c(v)$ were made nonlinear here, since these two terms must certainly change with input level.

[3]There is another discrepancy between the experimental results and the simulations in the overall shape of the patterns. For the range of frequency ratios observed here, we see a maximum in DPOAE level for human subjects at a frequency ratio around 1.225 (Gaskill and Brown, 1990) while the level is reduced for smaller and larger frequency ratios. This reflects the so-called ''second filter'' effect (e.g., Brown and Williams, 1993; Allen and Fahey, 1993), which is currently not included in our simulations. With the parameter settings used in this study, the second filter effect produced by the model does not resemble the shapes found in the experimental data. However, as described in van Hengel and Duifhuis (1999), the second filter behavior can also be simulated using this kind of transmission-line model. Therefore, in the near future attempts will be made to improve the model results by finding parameter values fitting both fine structure and the second filter.

Allen, J., and Fahey, P. (**1993**). ''A second cochlear-frequency map that correlates distortion product and neural tuning measurements,'' J. Acoust. Soc. Am. **94**, 809–816.

Brown, A. M., Harris, F. P., and Beveridge, H. A. (**1996**). ''Two sources of acoustic distortion products from the human cochlea,'' J. Acoust. Soc. Am. **100**, 3260–3267.

Brown, A., and Williams, D. (**1993**). ''A second filter in the cochlea'' in *Biophysics of Hair Cell Sensory Systems*, edited by J. H. Duifhuis, P. van Dijk, and S. M. van Netten (World Scientific, Singapore), pp. 72–77.

de Boer, E. (**1995**). ''The 'inverse problem' solved for a three-dimensional model of the cochlea. I. Analysis,'' J. Acoust. Soc. Am. **98**, 896–903.

Duifhuis, H., Hoogstraten, H. W., van Netten, S. M., Diependaal, R. J., and Bialek, W. (**1985**). ''Modelling the cochlear partition with coupled van der Pol-Oscillators,'' in *Peripherial Auditory Mechanisms*, edited by J. B. Allen, J. L. Hall, A. E. Hubbard, S. T. Neely, and A. Tubis, Lecture Notes in Biomathematics 64 (Springer, Berlin), pp. 290–297.

Furst, M., and Goldstein, J. L. (**1982**). ''A cochlear nonlinear transmission-line model compatible with combination tone psychophysics,'' J. Acoust. Soc. Am. **72**, 717–726.

Gaskill, S. A., and Brown, A. M. (**1990**). ''The behaviour of the acoustic distortion product, $2f1-f2$, from the human ear and its relation to auditory sensitivity,'' J. Acoust. Soc. Am. **88**, 821–839.

Gaskill, S. A., and Brown, A. M. (**1996**). ''Suppression of human acoustic distortion product: dual origin of $2f1-f2$,'' J. Acoust. Soc. Am. **100**, 3268–3274.

Greenwood, D. D. (**1991**). ''Critical bandwidth and consonance in relation to cochlear frequency-position coordinates,'' Hear. Res. **54**, 164–208.

Harris, F. P., Probst, R., and Xu, L. (**1992**). ''Suppression of the $2f1-f2$ otoacoustic emission in humans,'' Hear. Res. **64**, 133–141.

He, N., and Schmiedt, R. A. (**1993**). ''Fine structure of the $2f1-f2$ acoustic distortion product: changes with primary levels,'' J. Acoust. Soc. Am. **94**, 2659–2669.

He, N., and Schmiedt, R. A. (**1997**). ''Fine structure of the $2f1-f2$ acoustic distortion product: effects of primary level and frequency ratios,'' J. Acoust. Soc. Am. **101**, 3554–3565.

Heitmann, J., Waldmann, B., Schnitzler, H. U., Plinkert, P. K., and Zenner, H. P. (**1998**). ''Suppression of distortion product otoacoustic emissions (DPOAE) near $2f1-f2$ removes DP-gram fine structure—Evidence for a secondary generator,'' J. Acoust. Soc. Am. **103**, 1527–1531.

Kummer, P., Janssen, T., and Arnold, W. (**1995**). ''Suppression tuning characteristics of the $2f1-f2$ distortion-product otoacoustic emission in humans,'' J. Acoust. Soc. Am. **98**, 197–210.

Long, G. R., and Talmadge, C. L. (**1997**). ''Spontaneous otoacoustic emission frequency is modulated by heartbeat,'' J. Acoust. Soc. Am. **102**, 2831–2848.

Mauermann, M., Uppenkamp, S., and Kollmeier, B. (**1997a**). ''Zusammenhang zwischen unterschiedlichen otoakustischen Emissionen und deren Relation zur Ruhehörschwelle,'' in *Fortschritte der Akustik—DAGA 97*, edited by P. Wille (DEGA e.V., Oldenburg), pp. 242–243.

Mauermann, M., Uppenkamp, S., and Kollmeier, B. (**1997b**). ''Periodizität und Pegelabhängigkeit der spektralen Feinstruktur von Verzerrungsprodukt-Emissionen [Periodicity and dependence on level of the distortion product otoacoustic emission spectral fine-structure],'' Audiol. Akustik **36**, 92–104.

Mauermann, M., Uppenkamp, S., van Hengel, P., and Kollmeier, B. (**1999**). ''Evidence for the distortion product frequency place as a source of distortion product otoacoustic emission (DPOAE) fine structure in humans. II. Fine structure for different shapes of cochlear hearing loss,'' J. Acoust. Soc. Am. **106**, 3484–3491.

Ruggero, M. A., and Rich, N. C. (**1991**). ''Application of a commercially-manufactured Doppler-shift laser velocimeter to the measurement of basilar-membrane vibration,'' Hear. Res. **51**, 215–230.

Shera, C. A., and Zweig, G. (**1993**). ''Order from chaos: resolving the paradox of periodicity in evoked otoacoustic emissions,'' in *Biophysics of Hair Cell Sensory Systems*, edited by H. Duifhuis, J. W. Horst, P. van Dijk, and S. M. van Netten (World Scientific, Singapore), pp. 54–63.

Shera, C. A., and Guinan, J. J. (**1998**). ''Reflection emissions and distortion products arise from fundamentally different mechanisms,'' in Abstracts of the 21st ARO Midwinter Research Meeting, Abstract No. 344, p. 86.
Shera, C. A., and Guinan, J. J. (**1999**). ''Evoked otoacoustic emissions arise by two fundamentally different mechanisms: A taxonomy for mammalian OAEs,'' J. Acoust. Soc. Am. **105**, 782–798.
Smurzynski, J., Leonard, G., Kim, D. O., Lafreniere, D. C., and Jung, M. D. (**1990**). ''Distortion product otoacoustic emissions in normal and impaired adult ears,'' Arch. Otolaryngol. Head Neck Surg. **116**, 1309–1316.
Sun, X., Schmiedt, R. A., He, N., and Lam, C. F. (**1994a**). ''Modeling the fine structure of the 2 $f1-f2$ acoustic distortion product. I. Model development,'' J. Acoust. Soc. Am. **96**, 2166–2174.
Sun, X., Schmiedt, R. A., He, N., and Lam, C. F. (**1994b**). ''Modeling the fine structure of the 2 $f1-f2$ acoustic distortion product. II. Model evaluation,'' J. Acoust. Soc. Am. **96**, 2175–2183.
Talmadge, C. L., and Tubis, A. (**1993**). ''On modeling the connection between spontaneous and evoked otoacoustic emissions,'' in *Biophysics of Hair Cell Sensory Systems*, edited by H. Duifhuis, J. W. Horst, P. van Dijk, and S. M. van Netten (World Scientific, Singapore), pp. 25–32.
Talmadge, C. L., Tubis, A., Long, G. R., and Piskorski, P. (**1998**). ''Modeling otoacoustic emission and hearing threshold fine structure,'' J. Acoust. Soc. Am. **104**, 1517–1543.
Talmadge, C. L., Long, G. R., Tubis, A., and Dhar, S. (**1999**). ''Experimental confirmation of the two-source interference model for the fine structure of distortion product otoacoustic emissions,'' J. Acoust. Soc. Am. **105**, 275–292.
Uppenkamp, S., and Mauermann, M. (**1999**). ''Effect of frequency ratio $f2/f1$ on spectral fine structure of distortion product otoacoustic emissions,'' Br. J. Audiol. **33**, 87–88(A).
van Hengel, P. (**1993**). Comment to paper presented by Shera and Zweig (1993), in *Biophysics of Hair Cell Sensory Systems*, edited by H. Duifhuis, J. W. Horst, P. van Dijk, and S. M. van Netten (World Scientific, Singapore), p. 62.
van Hengel, P. W. J., Duifhuis, H., and van den Raadt, M. P. M. G. (**1996**). ''Spatial periodicity in the cochlea: the result of interaction of spontaneous emissions?'' J. Acoust. Soc. Am. **99**, 3566–3571.
van Hengel, P. W. J., and Duifhuis, H. (**1999**). ''The generation of distortion products in a nonlinear transmission line model of the cochlea,'' Proceedings of the Symposium on Recent Developments in Auditory Mechanics, 25–30 July 1999, Sendai, Japan.
van den Raadt, M. P. M. G., and Duifhuis, H. (**1990**). ''A generalized Van der Pol-oscillator cochlea model,'' in *The Mechanics and Biophysics of Hearing*, edited by P. Dallos, C. D. Geisler, J. W. Matthews, M. A. Ruggero, and C. R. Steele, Lecture Notes in Biomathematics 87 (Springer, Berlin), pp. 227–234.
van den Raadt, M. P. M. G., and Duifhuis, H. (**1993**). ''Different boundary conditions in a one-dimensional time domain model,'' in *Biophysics of Hair Cell Sensory Systems*, edited by H. Duifhuis, J. W. Horst, P. van Dijk, and S. M. van Netten (World Scientific, Singapore), p. 103.
Zweig, G. (**1991**). ''Finding the impedance of the organ of Corti,'' J. Acoust. Soc. Am. **89**, 1229–1254.
Zweig, G., and Shera, C. A. (**1995**). ''The origin of periodicity in the spectrum of evoked otoacoustic emissions,'' J. Acoust. Soc. Am. **98**, 2018–2047.